Unimolecular Chemistry of Protonated Formamide. Mass Spectrometry and *ab Initio* Quantum Chemical Calculations

Hung-Yu Lin,[†] Douglas P. Ridge,[†] Einar Uggerud,*[,‡] and Tore Vulpius[§]

Contribution from the Department of Chemistry and Biochemistry, University of Delaware, Newark, Delaware 19716, Department of Chemistry, University of Oslo, P.O. Box 1033 Blindern, N-0315 Oslo, Norway, and Department of Chemistry, H. C. Ørsted Institute, University of Copenhagen, DK-2100 Copenhagen, Denmark

Received February 25, 1993[⊗]

Abstract: The potential energy hypersurface of protonated formamide has been investigated. Using a dual-cell Fourier transform mass spectrometer, proton-transfer experiments with formamide were performed. From these experiments the activation energies for the three unimolecular reactions observed, (i) loss of water, (ii) loss of ammonia, and (iii) loss of carbon monoxide, were determined. Using a four-sector mass spectrometer, the fragmentations of metastable protonated formamide ions were observed. The results of all experiments, supported by high-level *ab initio* quantum chemical calculations and RRKM calculations, provide a consistent reaction model. The reaction paths for loss of water and loss of ammonia depart from the most stable O-protonated isomer, while the somewhat less stable N-protonated isomer is the precursor for CO loss. The significance of the gas-phase chemistry of protonated formamide to the solution phase is discussed.

Introduction

Peptide Hydrolysis. Protonation of carbonyl-containing compounds is of fundamental interest to organic chemistry. A number of important addition/elimination reactions are known to be acid catalyzed.[1] Among these reactions is the hydrolysis of amides and peptides. The initial step in amide hydrolysis is the attack of a proton:

$$BH^+ + RCONR'R'' = [RC(OH)NR'R'']^+ + B \quad (1a)$$

Formation of the protonated amide is essential in the acid-catalyzed hydrolysis mechanism. In contrast to the neutral amide, the oxygen-protonated species is sufficiently polar to be vulnerable to water attack in the actual hydrolysis step:

$$[RC(OH)NR'R'']^+ + H_2O = [RC(OH)(H_2O)NR'R'']^+ \quad (1b)$$

$$[RC(OH)(OH_2)NR'R'']^+ = [RC(OH)(OH)NHR'R'']^+ \quad (1c)$$

$$[RC(OH)(OH)NHR'R'']^+ = [RC(OH)(OH)]^+ + NHR'R'' \quad (1d)$$

When the reaction is conducted in a very strong acid, a shift in mechanism is sometimes observed.[2] The addition/elimination mechanism becomes unimportant, and an S_N1-type A-1 mechanism seems to take over. In this mechanism the amide is protonated on nitrogen and an acylium ion is formed in a unimolecular step (eq 2b). A water molecular then attacks the acylium ion.

$$BH^+ + RCONR'R'' = [RCONHR'R'']^+ + B \quad (2a)$$

$$[RCONHR'R'']^+ = [RCO]^+ + HNR'R'' \quad (2b)$$

$$[RCO]^+ + H_2O = [R(CO)OH_2]^+ \quad (2c)$$

When the protonation reaction is conducted in the gas phase, in the absence of solvent molecules, only the unimolecular chemistry of the protonated amide will be observed. The rate of fragmentation and the nature of the products formed depend intimately on the potential energy surface and on the internal energy acquired by the system in the protonation step. Knowledge about the kinetics, energetics, and mechanism of the gas-phase chemistry may therefore cast light on the solution-phase chemistry.

Protonation on N *vs* O. Proton exchange reactions of peptides and proteins have been studied for many years. Using various NMR techniques, Perrin[3] has shown that the acid-catalyzed proton exchange of peptides in an aqueous environment goes via a mechanism in which the imidic acid $[RC(OH)NR'R'']^+$ is an intermediate (O-protonation). The alternative route, N-protonation, is unimportant for peptides. However, N-protonation was shown to be important when the R-group is non-electron-withdrawing, for example when R = CH_3. However, relatively little is known about the intrinsic molecular properties of peptides and amides with respect to protonation. Again, insight can be obtained from gas-phase studies. It would be valuable to know if there is a preference for O-protonation *vs* N-protonation in the gas phase and how the two different isomers so formed react in following reactions.

Mass Spectrometric Fragmentation of Protonated Peptides. The introduction of desorption ionization methods for producing molecule–ions of involabile compounds has revolutionized the use of mass spectrometry in the biological sciences. Protonated peptides are formed in the gas phase when various ionization methods are used. These methods include fast atom bombardment (FAB/SIMS),[4] plasma desorption (PD),[5] laser desorption (LD),[6] electrospray ionization,[7] and field desorption (FD).[8] Mass

[†] University of Delaware.
[‡] University of Oslo.
[§] University of Copenhagen.
[⊗] Abstract published in *Advance ACS Abstracts*, March 1, 1994.

(1) (a) Lowry, T. H.; Richardson, K. S. *Mechanism and Theory in Organic Chemistry*, 3rd ed.; Harper & Row: New York, 1987. (b) Tates, K.; Modro, T. A. *Acc. Chem. Res.* **1978**, *11*, 190.
(2) Edward, J. T.; Derdall, G. D.; Wong, S. C. *J. Am. Chem. Soc.* **1978**, *100*, 7023.
(3) Perrin, C. L. *Acc. Chem. Res.* **1989**, *22*, 268.
(4) Barber, M.; Bordioli, R. S.; Sedwick, R. D.; Tyler, A. N. *J. Chem. Soc., Chem. Commun.* **1981**, 325.
(5) Jonsson, G. P.; Hedin, A. B.; Håkansson, P. L.; Sundquist, B. U.; Save, G. B. S.; Nielsen, P. F.; Roepstorff, P.; Johansson, K.-E.; Kamensky, I.; Lindberg, M. S. L. *Anal. Chem.* **1986**, *58*, 1084.
(6) Karas, M.; Hillenkamp, F. *Anal. Chem.* **1988**, *60*, 2299.
(7) Wong, S. F.; Meng, C. K.; Fenn, J. B. *J. Phys. Chem.* **1988**, *92*, 546.
(8) Beckey, H. D. *Field Ionization and Field Desorption Mass Spectrometry*, Pergamon Press: Oxford, 1978. See also: Schulten, H.-R.; Lattimer, R. P. *Mass Spectrom. Rev.* **1984**, *3*, 231.

0002-7863/94/1516-2996$04.50/0

analysis of protonated peptides provides important molecular weight information about the peptide under analysis. Furthermore, mass analysis of the fragments provides information about the molecular structure of the peptide. Formation of fragments can be enhanced by collisional activation or photoactivation of the protonated peptide. Unfortunately very little quantitative information exists about the energetics and mechanisms of the different fragmentation reactions observed for protonated peptides. This lack of knowledge is a serious obstacle for the full use of mass spectrometry in the analysis of peptides.

Scope. All three points mentioned above provide the motivation for the present work. The simplest molecule which contains the amide bond is formamide (M = $HCONH_2$). By using mass spectrometric methods in conjunction with theoretical methods, we decided to investigate the reactions initiated by proton transfer to this prototype peptide-like molecule. The questions we raise in this paper are (i) How is the pattern of fragmentation determined by the initial site of protonation? (ii) Which fragmentation channels are accessible at different energies? (iii) What are the precise barrier heights associated with the reactions observed? (iv) What is the barrier height associated with intramolecular rearrangement between the N-protonated and the O-protonated isomers, and how is this intramolecular proton transfer related to unimolecular fragmentation products observed?

To answer these questions we have investigated a series of proton-transfer reactions:

$$BH^+ + HCONH_2 = [(HCONH_2)H^+]^* + B \quad (3)$$

$$[(HCONH_2)H^+]^* \rightarrow \text{fragments} \quad (4)$$

The exothermicity of the proton-transfer reaction controls the internal energy deposited in protonated formamide. This in turn determines the products formed in the subsequent unimolecular fragmentation. By selecting the proton donors, BH^+, where the corresponding bases, B, have different proton affinities, the reactivity can be investigated as a function of internal energy. Using a Fourier transform mass spectrometer (FTMS) for the experiments provides two advantages as compared to a high-pressure chemical ionization mass spectrometer.[9] First, the collision rate is low compared to the rates of unimolecular reactions. This prevents ions from being collisionally deexcited before they can fragment. Second, by ejecting all ions but the proton donor prior to reaction, unwanted side reactions can be prevented.

In addition to the FTMS experiments we conducted measurements of the reactions of metastable MH^+ ions using a four-sector mass spectrometer. As the result of the long time delay between ion formation and reaction, metastable ions have total energies which are normally close to the potential energy barriers for fragmentation.[10] For this reason the appearance of a metastable ion spectrum is a very sensitive indicator of relative barrier heights for competing reactions.

Ab initio quantum chemical calculations can be extremely helpful in assigning ion fragmentation pathways. Model calculations at a high level of theory (MP2/6-31G**) were carried out to characterize structures of reactants, products, intermediates, and transition states and to obtain their potential energies. Experience has shown that calculations of this type provide relative energies which generally are within 20–30 kJ mol^{-1} of the corresponding experimental figures.[11]

To obtain a model in complete agreement with the experiments, it was necessary to adjust the quantum chemical barrier heights slightly. This was done using the RRKM method.[12]

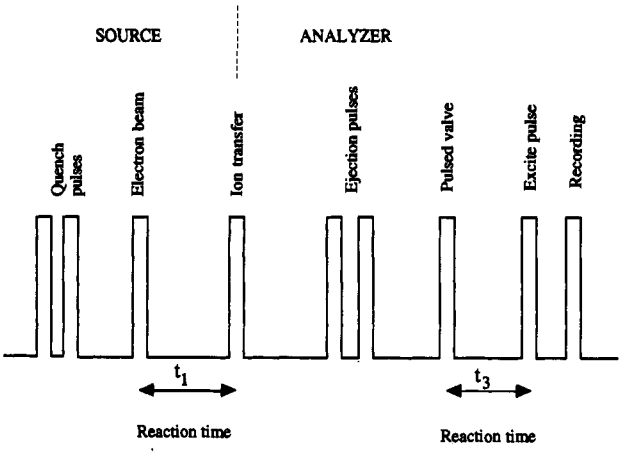

Figure 1. Pulse sequence used in the FTMS experiments.

Experimental Section

FTMS Study. The proton-transfer reactions were performed with a dual-cell Fourier transform mass spectrometer (FTMS-2000, Extrel Ltd., Madison, WI). The appropriate reactant gases were mixed in the source cell, and proton donor molecules, BH^+, were formed as the result of ion–molecule reactions initiated by a short 70-eV electron beam pulse. After a time delay, the proton donor molecules, BH^+, were transferred to the analyzer cell by opening the gate potential of the aperture plate between the two cells for a predetermined time. By careful choice of excitation pulse frequency widths and amplitudes, all ions, except the BH^+ ions, were ejected from the analyzer cell. Thereafter, a computer-controlled pulse valve was opened for a short time, allowing formamide to enter the analyzer cell. BH^+ and formamide were then allowed to react. The mass spectrum was recorded after a variable reaction time, t_3. In this way the product ion distribution could be obtained as a function of time. The pulse sequence used is shown in Figure 1. The instrument was operated at sufficiently high resolution to identify all reactants and products by precise mass measurement. Typically ions were kept in the source cell for 0.3–1.0 s at a total pressure of ca. 3×10^{-7} Torr. This corresponds to enough time for three to ten collisions or symmetric charge transfers. Product distributions on reaction with formamide in the analyzer cell were independent of this storage time.

Metastable Ion Study. Protonated formamide ions (MH^+, m/z 46) were produced by chemical ionization in the ion source of a four-sector mass spectrometer (JMS-HX/HX 110 A, Jeol Ltd., Tokyo, Japan). The reagent gases used were either H_2 or CH_4. The acceleration voltage was 10 kV. Using the first two sectors (E and B), only ions with nominal m/z 46 were allowed to enter the third field-free region of the instrument. The product ions which were formed by unimolecular fragmentation of MH^+ ions in the third field-free region were recorded in the form of a MIKE spectrum by scanning the voltage of the third (E) sector of the instrument. The lifetime of the m/z 46 metastable ions which decompose in the third field-free region is approximately 13–22 μs in this instrument.

All reactants were of commercial grade and were checked for purity using both electron impact ionization (EI) and chemical ionization (CI).

Methods of Calculation

***Ab Initio* Study.** The program systems GAUSSIAN 86, GAUSSIAN 88, and GAUSSIAN 92[13] were used for the calculations. The molecular geometries of all species relevant to the unimolecular chemistry of protonated formamide were first optimized using the 4-31G basis set[14] at the Hartree–Fock (HF) level of theory.[15] Start geometries for the transition-state

(9) Freiser, B. S. In *Techniques for the Study of Ion-Molecule Reactions*; Farrar, J. M., Saunders, W. H., Jr., Eds.; John Wiley: New York, 1988.

(10) Cooks, R. G.; Beynon, J. H.; Caprioli, R. M.; Lester, G. R. *Metastable Ions*; Elsevier: Amsterdam, 1973.

(11) (a) Boyd, D. B. In *Reviews in Computational Chemistry*; Lipkowitz, K. B., Boyd, D. B., Eds.; VCH Publishers: New York, 1990. (b) Minkin, V. I.; Simkin, B. Ya.; Minyaev. *Quantum Chemistry of Organic Compounds*; Springer-Verlag: Berlin, 1990.

(12) Forst, W. *Theory of Unimolecular Reactions*; Academic Press: New York, 1973.

(13) Frisch, M. J.; Trucks, G. W.; Head-Gordon, M.; Gill, P. M. W.; Wong, M. W.; Foresman, J. B.; Johnson, B. G.; Schlegel, H. B.; Robb, M. A.; Replogle, E. S.; Gomperts, R.; Andres, J. L.; Raghavachari, K.; Binkley, J. S.; Gonzalez, C.; Martin, R. L.; Fox, D. J.; Defrees, D. J.; Baker, J.; Stewart, J. J. P.; Pople, J. A. *GAUSSIAN 92*, Gaussian Inc.: Pittsburgh, PA, 1992.

(14) Hehre, W. J.; Ditchfield, R.; Pople, J. A. *J. Am. Chem. Soc.* **1972**, *56*, 2257.

(15) Roothan, C. C. *J. Rev. Mode. Phys.* **1951**, *23*, 69.

Table 1. Proton Transfer Reaction Data (kJ mol^{-1}) Taken from Ref 20

molecule (M)	$\Delta H^{\circ}_{f,298}$(M)	$\Delta H^{\circ}_{f,298}$(MH^+)	PA (M)	ΔPA	obsd CO loss	obsd H_2O loss	obsd NH_3 loss
$HCONH_2$	−186	514	830	0			
CH_2CO	−61	657 (653)[a]	828	2	no	no	no
C_2H_4	52	902	680	150	no	no	no
CH_4	−74	905	551	279	yes	no	no
Cl	122	1138	514	316	yes	no	no
N_2	0	1036	495	335	yes	yes	yes
O_2	0	1106	424	406	yes	yes	yes
H_2	0	1106	424	406	yes	yes	yes

[a] Value in parentheses is from AE measurements.

optimizations were obtained by the linear synchronous transit method.[16] For one case (TS1) this approach failed and a crude guess of the start geometry proved to be successful. A combination of the Newton algorithm and normal coordinate-following algorithms was used for the transition-state optimizations. The optimized geometries were checked for the correct number of negative eigenvalues of the Hessian (the second-derivative matrix). Analytical force constants were computed at this stage, and the vibrational frequencies were obtained. These vibrational frequencies were used for the final zero-point vibrational energy correction after scaling by a factor of 0.9. The 4-31G geometries were used as the start geometries for the final stage of the optimizations. At this stage the wave functions were calculated using the Möller–Plesset perturbation theory to the second order[17] with a 6-31G** basis set.[18] The optimized MP2/6-31G** geometries and energies together with the HF/4-31G zero-point energies provide the final results.

RRKM Study. A standard computer procedure was employed for the RRKM calculations. The method has been developed by us to incorporate quantum mechanical barrier tunneling.[19] The scaled normal frequencies of vibration from the *ab initio* calculations were used as input. The reaction barrier height of one particular reaction (TS3) was the only variable in these calculations. Starting with the *ab initio* value, the height was adjusted to give a best overall fit with the experimentally observed product distributions (branching ratios).

Results and Discussion

In the FTMS experiments the following proton (deuteron) donors were investigated (listed in order of decreasing proton affinity of the corresponding neutral base): $C_2D_5^+$, CD_5^+, DCl^+, N_2D^+, and O_2D^+. The general reaction scheme is Table 1 lists

$$BD^+ + HCONH_2 \rightarrow (HCONH_2)D^+ (m/z\ 47) + B \quad (5)$$

$$\rightarrow NH_3D^+ (m/z\ 19) + CO + B \quad (6)$$

$$\rightarrow HCNH^+ (m/z\ 28) + HDO + B \quad (7)$$

$$\rightarrow HCO^+ (m/z\ 29) + NH_2D + B \quad (8)$$

the proton transfer reaction data.[20] The use of deuterated reactant ions was necessary for a unique identification of product ion structures and in order to reveal possible interfering hydrogen exchange reactions.

Secondary Reactions. As reaction time increases, secondary reactions produce $(HCONH_2)H^+$. Among these are

$$(HCONH_2)D^+ + HCONH_2 \rightarrow (HCONH_2)H^+ (m/z\ 46) + HCONHD \quad (9)$$

and proton transfer from the primary products $HCNH^+$ and HCO^+. It was always possible to correctly identify the products of a reaction by sampling at delay times corresponding to a small extent of conversion of primary reactant to products.

Efforts to eliminate water from the system were not completely successful, so H_2O^+ (m/z 18) is formed by electron impact, H_3O^+ (m/z 19) is formed by proton transfer, and DH_2O^+ (m/z 20) is formed by deuteron transfer from BD^+. These ions were identified by accurate mass measurements. In a secondary reaction DH_2O^+ can transfer a proton or a deuteron to formamide. Water has a proton affinity too low for it to react with $HCNH^+$ or NH_3D^+ and too high for DH_2O^+ to react with formamide to produce $HCNH^+$, HCO^+, or NH_3D^+. The product ion HCO^+ will transfer its proton to water, which makes determination of the relative abundance of this ion relative to the other product ions difficult. The only effect of the presence of water on the relative abundance of the products of reactions 5–7 is to decrease the relative amounts of HCO^+ and $(HCONH_2)D^+$ at longer reaction times, but it does not prevent correct identification of the products of reactions 5–8.

Deuteron Transfer from DCl^+. In the case of DCl, a significant amount of HCl is formed by H/D exchange in the inlet system even after it has been "deuterated" by overnight exposure to DCl. Observation at a short reaction time still assures correct identification of the products after reaction with DCl^+. The mass spectra obtained after reaction times $t_3 = 0.1$ s and $t_3 = 0.6$ s are shown in Figure 2. The peaks at m/z 37 and m/z 39 correspond to DCl^+ and those at m/z 36 and m/z 38 to HCl^+. The relatively large amount of HCl^+ comes from H/D exchange of neutral DCl in the inlet system and from charge exchange between HCl and DCl^+ in the source. The large peak at m/z 45 is attributed to the following charge exchange process:

$$DCl^+ + HCONH_2 \rightarrow HCONH_2^+ (m/z\ 45) + DCl \quad (10)$$

This reaction is exothermic by 250 kJ mol^{-1} (the difference in ionization energies between $HCONH_2$ and DCl). $HCONH_2^+$ reacts fast in the following self-CI process to produce $(HCONH_2)H^+$:

$$HCONH_2^+ + HCONH_2 \rightarrow (HCONH_2)H^+ (m/z\ 46) + (C,H_2,N,O) \quad (11)$$

The deuteron-transfer product $(HCONH_2)D^+$ (m/z 47) is observed at short reaction times, but diminishes somewhat at longer times, probably as a result of H/D exchange via reaction 9. The peak at m/z 19 is a doublet (unresolved in the reproduced spectra). The peak at m/z 19.018 can be ascribed to H_3O^+, and the peak at m/z 19.041 to NH_3D^+. The latter ion is a reaction product from $(HCONH_2)D^+$.

Deuteron Transfer from CD_5^+. In the reaction between CD_5^+ and formamide (spectrum not shown here) a small peak corresponding to NH_3D^+ was also observed. This observation makes it possible to determine an upper limit of the activation energy of the following reaction:

(16) Halgren, T. A.; Lipscomb, W. M. *Chem. Phys. Lett.* **1977**, *49*, 225.
(17) Möller, C.; Plesset, M. S. *Phys. Rev.* **1934**, *46*, 618.
(18) Frisch, M. J.; Pople, J. A.; Binkley, J. S. *J. Chem. Phys.* **1984**, *80*, 3265.
(19) Hvistendahl, G.; Uggerud, E. *Org. Mass Spectrom.* **1991**, *26*, 67.
(20) Lias, S. G.; Bartmess, J. E.; Liebman, J. F.; Holmes, J. H.; Levin, R. D.; Mallard, W. G. *Gas-Phase Ion and Neutral Thermochemistry. J. Phys. Chem. Ref. Data* **1988**, *17*, Suppl. 1.

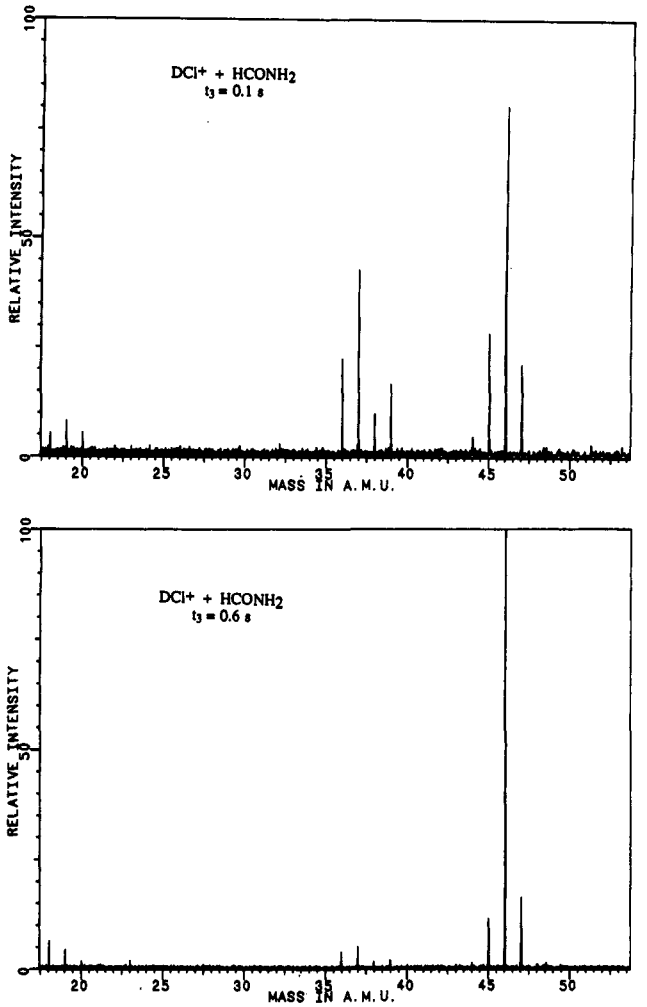

Figure 2. Mass spectrum obtained after (a) t_3 = 0.1 s and (b) t_3 = 0.6 s in the reaction between DCl^+ and formamide.

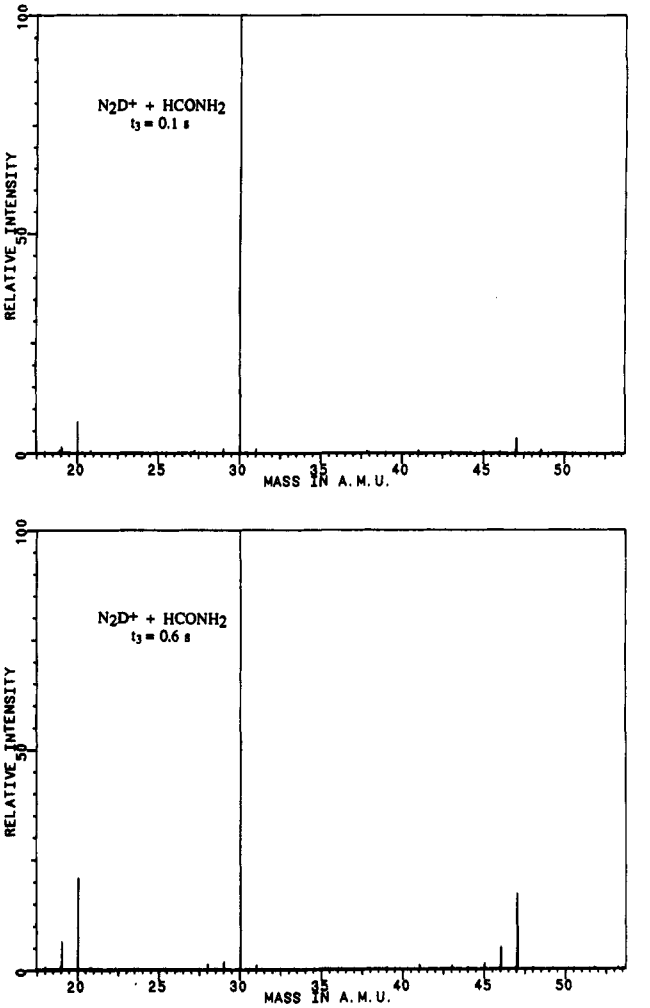

Figure 3. Mass spectrum obtained after (a) t_3 = 0.1 s and (b) t_3 = 0.6 s in the reaction between N_2D^+ and formamide.

$$(HCONH_2)H^+ \rightarrow NH_4^+ + CO \qquad (12)$$

Using the data for CH_5^+ (Table 1) gives $E_{act} < 279$ kJ mol^{-1} for reaction 12.

Deuteron Transfer from N_2D^+. The spectra are shown in Figure 3. The peak at m/z 30 corresponds to N_2D^+, and the ion with m/z 29 corresponds to N_2H^+. Charge exchange is also observed in this system; the peak at m/z 45 corresponds to $HCONH_2^+$ formed in the following dissociative charge exchange reaction:

$$N_2D^+ + HCONH_2 \rightarrow HCONH_2^+ (m/z\ 45) + N_2 + D \qquad (13)$$

which is exothermic by 162 kJ mol^{-1}. The observation of a peak at m/z 20 (H_2DO^+) shows that water is present in the system. The NH_3D^+ ion with m/z 19.041 is substantial in this case, showing that many $(HCONH_2)D^+$ ions are formed with internal energy well above the dissociation threshold for CO loss. The small peaks at m/z 28.019 and m/z 29.003, corresponding to $HCNH^+$ and HCO^+, are formed in the processes

$$(HCONH_2)D^+ \rightarrow HCNH^+ + DHO \qquad (14)$$

$$(HCONH_2)D^+ \rightarrow HCO^+ + NH_2D \qquad (15)$$

Using the data for N_2H^+ (Table 1) gives $E_{act} < 335$ kJ mol^{-1} for both reactions 14 and 15.

Deuteron Transfer from O_2D^+. The spectra are shown in Figure 4. The spectra contain peaks due to charge exchange with formamide and to proton transfer to water. The peak at m/z 34 corresponds to O_2D^+. The dissociative charge transfer

$$O_2D^+ + HCONH_2 \rightarrow HCONH_2^+ (m/z\ 45) + O_2 + D \qquad (16)$$

is exothermic by 92 kJ mol^{-1}. The peaks at m/z 19.041, m/z 28.019, and m/z 29.003 correspond to NH_3D^+, $HCNH^+$, and HCO^+, respectively. This shows that the reactions in which these ions are formed occur well above the thermochemical threshold. The peak at m/z 30.020 is identified to be due to N_2D^+ and *not* DCO^+ (m/z 30.010). This finding suggests that loss of ammonia does not occur by a mechanism which involves H/D scrambling.

Energy Transfer upon Protonation. Before discussing further the significance of the findings from the FTMS experiments, one important methodological problem has to be addressed. This problem concerns the uncertainty about the exact amount of energy deposited in the protonated formamide molecules.

The detailed mechanisms of the proton-transfer reactions are not known. In principle, it is possible to distinguish between two limiting cases. In the first mechanism the proton is transferred from the donor to the acceptor in a long-lived collision complex. In the second mechanism the proton is stripped off the donor in a direct collision.

We will first consider the collision-complex mechanism.[21] The conventional formulation of this mechanism involves a double-well potential. A proton-bound dimer, $(BH\cdots M)^+$, is initially formed between the donor and acceptor. This complex will either fall apart to reform the reactants or it will rearrange to give the complex $(B\cdots HM)^+$:

$$BH^+ + M = (BH\cdots M)^+ = (B\cdots HM)^+ = B + MH^+ \qquad (17)$$

If the complex $(B\cdots MH)^+$ exists for several rotational periods

(21) See for example: Lias, S. G. *J. Chem. Phys.* **1984**, *88*, 4401.

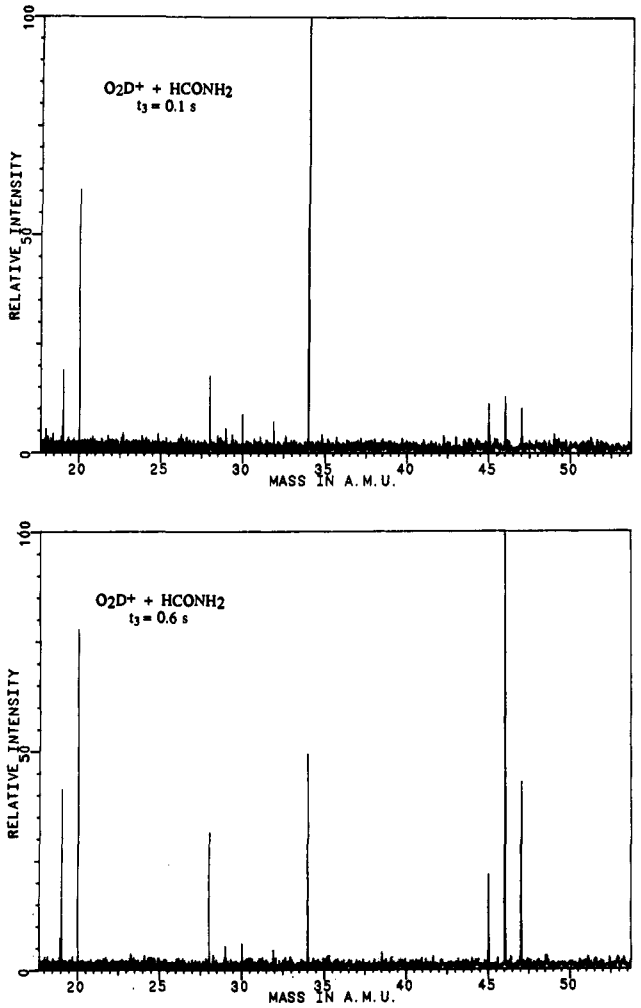

Figure 4. Mass spectrum obtained after (a) $t_3 = 0.1$ s and (b) $t_3 = 0.6$ s in the reaction between O_2D^+ and formamide.

before it breaks apart to form the products, it can roughly be assumed that the energy in the products is statistically distributed among all internal degrees of freedom. For the complex to be sufficiently long-lived there must be a barrier toward product formation. This is usually the case for weakly exothermic and thermoneutral proton-transfer reactions. The existence of a long-lived collision complex for strongly exothermic reactions, like those studied in the present work, is less likely. For such reactions there is no barrier for the reaction, and the reaction will proceed via the direct stripping mechanism.

In this mechanism the proton is transferred from the donor to the acceptor *en passant*, without the formation of a long-lived collision complex. The internal energy of MH^+ ions formed in a stripping mechanism can in general not be calculated from statistical theories because the energy transferred is determined by the detailed reaction dynamics of the individual systems. Exothermic proton-transfer reactions between halogenides have been studied using infrared chemiluminescence.[22] From the analysis of these experiments it was concluded that the average energy transferred is large, but in no instance was the energy transfer 100%. From the results of proton-transfer reactions to C_3H_6O compounds it was concluded that the average internal energy of the MH^+ ions was roughly half of the reaction exothermicity.[23] However, the internal energy distribution has a long tail, and a small amount of the ions seemed to have an internal energy close to 100% of the reaction exothermicity.

So far it has been assumed that all reactant ions are thermal. Ions which are trapped in an FTMS cell may possess excess kinetic and/or internal energy. As noted above, however, product distributions are not sensitive to the number of collisions the reactant ions suffer in the source before it is transferred to the analyzer and exposed to neutral formamide. This suggests that the reactions observed are not driven by excess energy of the reactant ions.

From this discussion it is clear that our FTMS experiments provide reasonable rigorous upper limits to the barrier for the reaction in question. The absence of a particular fragmentation initiated by a proton-transfer reaction with a known exothermicity, however, does not necessarily mean that the barrier for the fragmentation reaction is higher than this exothermicity. Thus lower limits on activation energies determined from the FTMS experiments are only suggestive, and more precise determinations of lower limits from MIKE spectra are desirable.

Metastable Ion Spectra. When CH_4 is used as reagent gas, little fragmentation is seen to occur in the ion source, as was evident from the normal mass spectrum. This is in agreement with the FTMS data. More fragmentation was observed with H_2, as could be expected from the higher acidity of H_3^+ as compared to CH_5^+. The MIKE spectra of metastable MH^+ ions (m/z 46) are shown in Figure 5. It is interesting to notice that all three product ions are observed when both CH_4 and H_2 are used, which points to a long high-energy tail of the MH^+ energy distribution function, although of course only a very small fraction of the ions are formed with energies in the range necessary for producing $HCNH^+$ and HCO^+. It should be remembered that the MIKE spectra only reflect the reactivity of the population of parent ions which have survived some 13 μs or more after ion formation and are therefore only reminiscent of the initial energy distribution. The absence of loss of water and ammonia in the FTMS experiments (proton donor CD_5^+) and the observation of the same reactions from metastable MH^+ ions are not in contradiction. The proportion of products from metastable MH^+ ions to stable MH^+ was measured to be *ca.* 10^{-6}, which is far below the noise level of the FTMS experiment.

The translational energy releases were determined from the individual peak widths after correcting for the width of the main ion beam. In both cases (CH_4 and H_2) the values were the same: NH_4^+ ($T_{0.5} = 0.12$ eV), $HCNH^+$ ($T_{0.5} = 0.29$ eV), and HCO^+ ($T_{0.5} = 0.27$ eV). It is reasonable to assume (see the following section on RRKM calculations) that the metastable MH^+ ions observed here fragment close to the energy thresholds of the respective reactions. Each of the translational energy releases can therefore be used to obtain an approximate lower limit on the energy difference between the transition state and the products of that reaction. Using the *experimentally* known heats of formation of the products (last column of Table 2) relative to protonated formamide, the following lower limits for the energies of the transition state for formation of NH_4^+ (17 kJ mol^{-1}), $HCNH^+$ (219 kJ mol^{-1}), and HCO^+ (292 kJ mol^{-1}) are obtained.

The relative proportion $[HCNH^+]:[HCO^+]$ is very close to 2 in both cases, although the amount of NH_4^+ varies by a factor of 6. This may indicate that NH_4^+ is formed from a different precursor than $HCNH^+$ and HCO^+ and that the relative amount of the two precursors varies with the nature of the protonating agent. A consequence of this is that formation of $HCNH^+$ and HCO^+ must have very similar energetic requirements, a finding which is in complete accord with the FTMS results. Moreover, the somewhat higher abundance of $HCNH^+$ points to a slightly lower barrier for the process leading to this ion.

Despite the fact that the pressure in the analyzer region is approximately $p = 10^{-8}$ mbar we were concerned about the possibility of collisional activation which otherwise could interfere with our quantitative measurements. Because of the very low relative abundance of metastable to stable MH^+ ions in this case (measurement of the ratio yields $[m/z = 18]:[m/z = 46] = 1.4 \times 10^{-6}$), the system could be suspected to be especially vulnerable. The presence of the small peaks at m/z 17 and m/z 27

(22) (a) Zwier, T. S.; Bierbaum, V. M.; Ellison, G. B.; Leone, S. R. *J. Chem. Phys.* **1980**, *72*, 5426. (b) Weisshaar, J. C.; Zwier, T. S.; Leone, S. R. *J. Chem. Phys.* **1981**, *75*, 4873.

(23) Bowen, R. D.; Harrison, A. G. *Org. Mass Spectrom.* **1981**, *16*, 159.

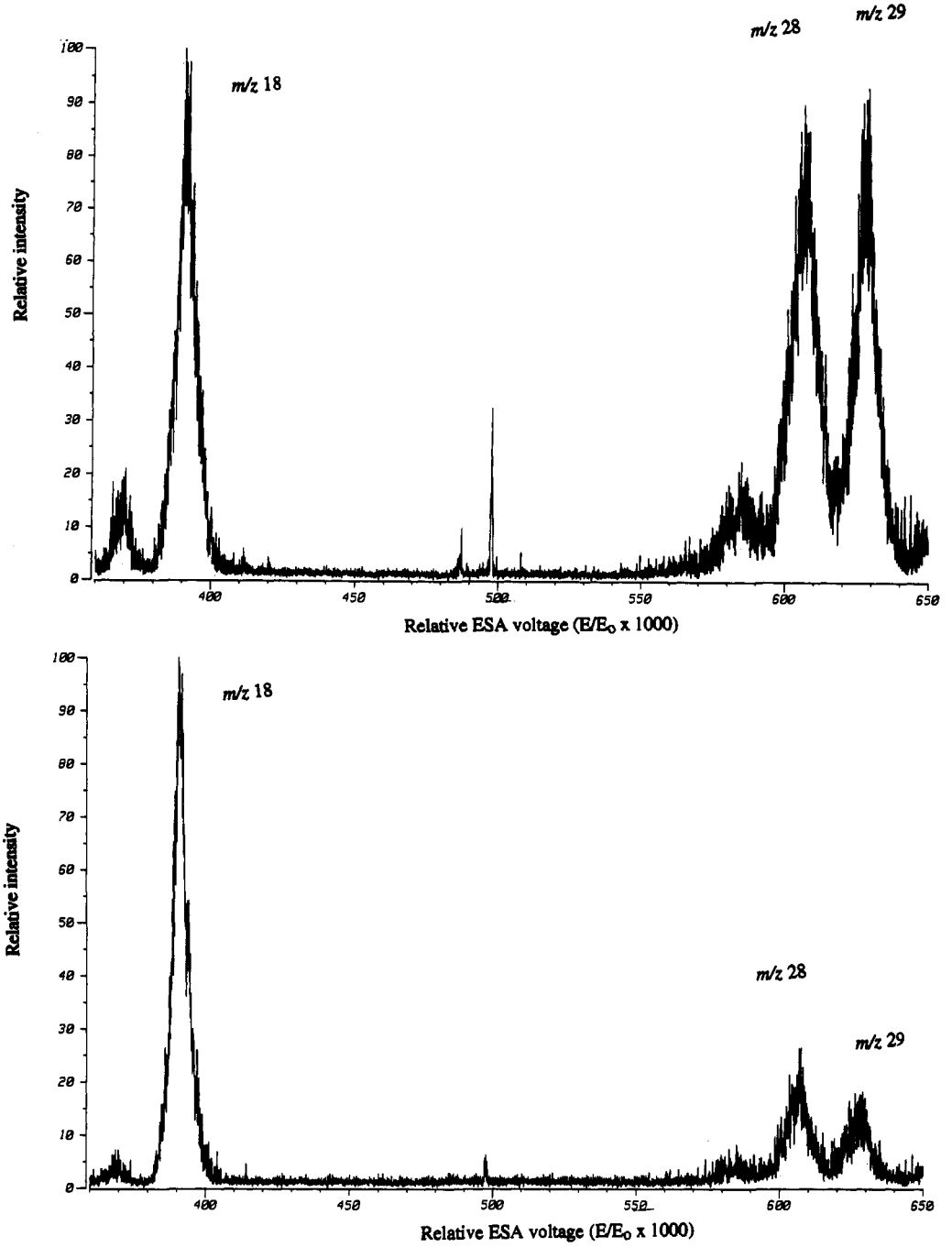

Figure 5. MIKE spectra of m/z 46 from chemical ionization of formamide when the CI gas is (a, top) CH_4 (proton donors are mainly CH_5^+ and $C_2H_5^+$) and (b, bottom) H_2 (proton donor is H_3^+).

strengthened this suspicion. By comparison with the collisional activation spectrum (obtained by letting air into the analyzer tube), it was possible to estimate the contribution of collisional activation to be less than approximately 5%.

***Ab Initio* Reaction Model.** The results of the quantum chemical calculations are summarized in Table 2, and the geometries of the transition states are shown in Figure 6. The calculations show that the O-protonated isomer, **2**, is 60 kJ mol^{-1} more stable than the N-protonated isomer, **3**. This is in agreement with experiment. It has been shown that the gas-phase proton affinities of amides can be expressed as a linear function of O_{1s} binding energies (as determined by ESCA) and first ionization energies.[24] Formamide fits well in this correlation. It was shown that O-protonation is slightly favored over N-protonation according to the data analysis. Our own labeling experiments turned out to be inconclusive regarding the site of protonation.[25] A simple electronic structure argument may be put forward to rationalize the difference in stabilities; the N-protonated form of an amide has only one mesomeric structure, while the O-protonated form has two. It should be mentioned also that semiempirical

(24) Catalán, J.; Mó, O.; Pérez, P.; Yáñez, M. *J. Chem. Soc., Perkin Trans. 2* **1982**, 1409.

(25) Deuteron transfer from CD_3CO^+ to formamide is almost thermoneutral. Therefore only the thermodynamically most favored isomer of $(HCONH_2)D^+$ will be formed in a deuteron-transfer experiment. The native idea of the experiment was that if this isomer is the O-protonated isomer, only D^+ is transferred in the subsequent reaction between $(HCONH_2)D^+$ and $HCONH_2$. If the N-protonated isomer is the more stable, the D and the two H's become equivalent prior to the proton transfer, and H/D exchange between the formamide molecules would be observed. In fact the experiments showed a very fast H/D exchange. However, this does not necessarily prove N-protonation. There is a more plausible explanation for the H/D exchange than the one offered above. The proton transfer between protonated formamide and formamide is thermoneutral, which implies the formation of a long-lived collision complex between the two reactants. This collision complex is known to be strongly bonded, probably between 80 and 100 kJ mol^{-1}. The energy gained upon formation of the complex is therefore sufficient to overcome the energy difference between the N- and the O-protonated forms, and H/D exchange will be the result. (For more mechanistic details see: Lias, S. G. *J. Phys. Chem.* **1984**, *88*, 4401.)

Table 2. Calculated Energy Data

molecule(s)	energy[a] (hartree)	E(zpv)[b] (kJ mol^{-1})	E(rel)[c] (kJ mol^{-1})	$\Delta\Delta H°$[d] (kJ mol^{-1})
$HCONH_2 + H^+$ (1)	−169.432 58	119	849	830
$HCOHNH_2^+$ (2)	−169.768 80	153	0	0
$HCONH_3^+$ (3)	−169.744 64	150	60	
NH_4^+···CO (4)	−169.782 10	146	−42	
NH_4^+···OC (5)	−169.775 07	144	−25	
$HCOH_2NH^+$ (6)	−169.691 92	141	190	
$HCNH^+$···OH_2 (7)	−169.738 13	127	55	
H_2O···$HCNH^+$ (8)	−169.720 30	134	108	
HCO^+ (9)	−113.272 32	42		
NH_3 (10)	−56.386 92	86		
9 + 10	−169.659 24	128	263	266
NH_4^+ (11)	−56.737 65	126		
CO (12)	−113.028 18	12		
11 + 12	−169.765 83	138	−7	5
$HCNH^+$ (13)	−93.457 30	73		
H_2O (14)	−76.222 45	53		
13 + 14	−169.679 75	126	207	191
TS1 (3 → 11 + 12)	−169.704 71	136	151	≤279; ≥17
TS2 (2 → 13 + 14)	−169.667 64	134	247	≤335; ≥219
TS3 (2 → 3)	−169.677 09	135	226	≤335; ≥292

[a] Energy obtained from optimized MP2/6-31G** structures. [b] Zero-point vibrational energies. Vibrational frequencies were calculated at HF/4-31G-optimized structures and scaled by a factor of 0.9. [c] Energy relative to 2. [d] Experimental difference in heats of reaction (relative to 2). For stable species the data have been taken from ref 20, while the transition-state energies are from this work. Consult text for details about how the upper and lower limits to the transition-state energies were obtained.

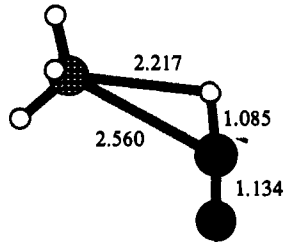

TS1

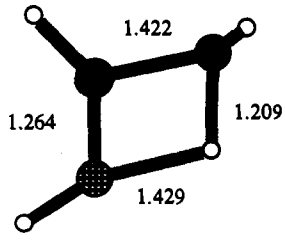

TS2

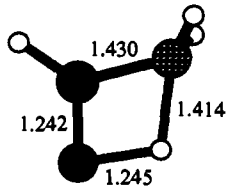

TS3

Figure 6. Transition-state structures (MP2/6-31G**). The most important bond distances are given in angstrom units. Filled (black) circles represent carbon atoms, open circles are hydrogens, filled (gray) circles are oxygens, and filled (wallpaper pattern) circles are nitrogens.

MINDO/3 calculations predict the O-protonated formamide to be the more stable isomer.[26]

Using the data from Table 2, the proton affinity of formamide is calculated to PA_{calc} = 849 kJ mol^{-1}. This figure is close to the experimental proton affinity PA_{exp} = 830 kJ mol^{-1}.

Our *ab initio* calculations indicate a substantial barrier (226 kJ mol^{-1}) for the rearrangement between the two isomers. This means that although there is a thermodynamic preference for the O-protonated isomer, the barrier will prevent rearrangement of a large part of the N-protonated molecules once they have been formed (*vide infra*).

Two reaction channels are open for energetic O-protonated formamide. It may either rearrange to the N-protonated isomer or it may fragment via the $[HC(OH_2)NH]^+$ isomer, **6**, to give $HCNH^+$ and H_2O. The reaction products are calculated to be 207 kJ mol^{-1} higher in energy than the reactant, in good agreement with the difference in the experimental heats of formation, which is 191 kJ mol^{-1} (Table 2). The calculated fragmentation barrier is 247 kJ mol^{-1}. From Table 2 it is seen that the high level of theory applied in the calculations gives energy differences between reactants and products in very good agreement with experimentally known differences in heats of formation. The deviations are on an average ±14 kJ mol^{-1}, and the deviation is in no instance larger than ±19 kJ mol^{-1}. This suggests that the calculated barrier heights are also quite reliable, although the error is likely to be higher than in the case of stable structures.

The calculated barrier heights for the water elimination and the isomerization are well below the upper limit of the activation energy of 355 kJ mol^{-1} deduced from the observation of reaction 14 and 15 when N_2D^+ is reacted with formamide (the FTMS experiment). The calculated barrier is seen to be closer to the estimate of the lower limit of 219 kJ mol^{-1} from the metastable ion experiment.

As already discussed the energy deposited in MH^+ cannot be expected to be 100% of the difference in proton affinity of formamide and the corresponding base of the proton donor. The failure of the DCl^+ reaction to give water loss illustrates this point. The FTMS results suggest that the internal energy deposited in deuterated formamide by the reaction is less than the barrier for water loss, for which the *ab initio* value is 247 kJ mol^{-1}. This is significantly less than the difference in proton affinity between Cl and formamide, which is 319 kJ mol^{-1}.

The N-protonated formamide $[HCONH_3]^+$ ion, **3**, can either (in principle) rearrange to the O-protonated isomer or fragment via the $[NH_4$···$CO]^+$ ion, **4**, to give NH_4^+ and CO. According to the calculations, the products are 7 kJ mol^{-1} lower in energy than the O-protonated isomer, **2**, while the experimental data show that they are 5 kJ mol^{-1} higher (Table 2). The barrier for this fragmentation is calculated to be 151 kJ mol^{-1} compared to **2**. Such a barrier is consistent with the fact that $C_2H_5^+$ with the potential to deposit as much as 150 kJ mol^{-1} in protonated formamide fails to give CO loss. The required experimental upper limit to the barrier is 279 kJ mol^{-1}, deduced from the observation of CO loss in the CD_5^+ reaction. The observation of CO loss in the CD_5^+ reaction is thus consistent with the calculated barrier of 151 kJ mol^{-1}. A rather long high-energy tail of the internal energy distribution when CH_5^+ is used as protonating agent can be inferred from the metastable ion spectrum of Figure 5a because in addition to NH_4^+ both $HCNH^+$ and HCO^+ are observed. This corresponds to MH^+, which has acquired beyond 247 kJ mol^{-1}, which is close to 100% of the theoretical maximum.

In principle, an alternative reaction path is open to the N-protonated formamide ion. Heat of formation data show that the products of this reaction, HCO^+ and NH_3, are 266 kJ mol^{-1} higher in energy than **2**. The corresponding calculated energy difference is 263 kJ mol^{-1}. The energy difference between these products and those actually observed (CO and NH_4^+) corresponds to the difference in proton affinity between NH_3 and CO. Although formation of HCO^+ would require a simple direct bond

(26) Tsitadze, G. V.; Zhidomirov, G. M.; Kvezereli, E. A.; Pel'menchikov, A. G.; Zhanplisov, N. U.; Meladze, M. A. *Izv. Akad. Nauk SSSR, Ser. Khim.* **1985**, 2617.

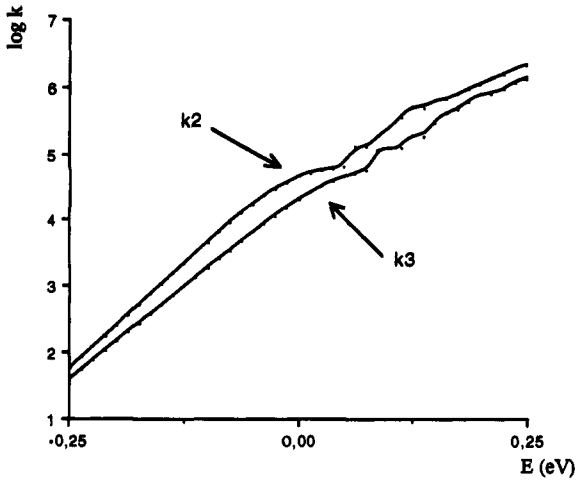

Figure 7. Rate *vs* energy curve for loss of water (k_2) and loss of ammonia (k_3) from protonated formamide obtained from RRKM calculations. The energy scale is set relative to the transition state for loss of water.

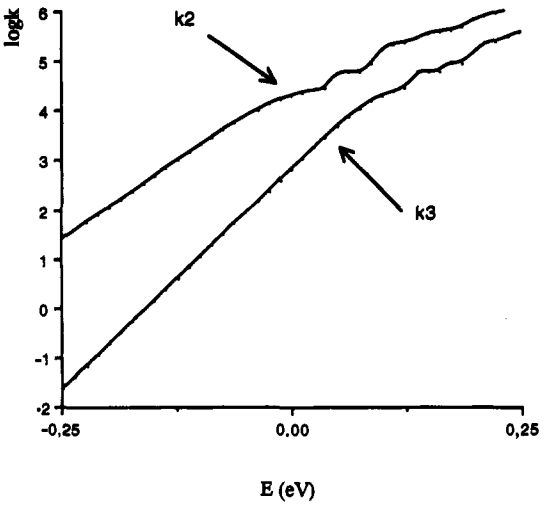

Figure 8. Rate *vs* energy curve for loss of HDO (k_2) and loss of NH_2D (k_3) from O-deuterated formamide obtained from RRKM calculations. The energy scale is set relative to the transition state for loss of water.

scission of $[HCONH_3]^+$, only the energetically more feasible rearrangement/fragmentation leading to NH_4^+ is observed. The calculations show that, in the initial phase of the fragmentation, the C–N bond is considerably stretched out. This motion would if it went on to infinity lead to elimination of ammonia. However, before the fragments depart, the proton is efficiently captured by NH_3, and only NH_4^+ is produced.

RRKM Calculations. So far, nothing has been stated with regard to the fate of O-protonated molecules, **2**, which rearrange into the valley of the N-protonated molecule, **3**, of the potential energy hypersurface. In principle, two fragmentation routes are open to the energetic N-protonated molecules so formed. They may produce either HCO^+ or NH_4^+. It is observed both from the FTMS and the metastable ion experiments that HCO^+ is formed in competition with $HCNH^+$. This can be understood if it is postulated that all ions which rearrange from **2** to **3** fragment to give HCO^+. In this connection it is important to realize that the *ab initio* barrier heights should not be taken as absolute. The calculated barrier height difference between TS2 and TS3 is only 21 kJ mol^{-1}. Even at the high level of theory employed this cannot be considered significant. In order to get a quantitatively more correct relationship between TS2, TS3, and the other species involved, we carried out a series of RRKM calculations.

The normal coordinate analysis shows that the main contribution to the reaction coordinates of both TS2 and TS3 is from the respective migrating hydrogen atom. For this reason it was prerequisite to include tunneling. This explains why the rate curves presented in Figures 7 and 8 extend to energies below the classical threshold.

The potential energy of TS3 was first adjusted to 289 kJ mol^{-1}, which is the *ab initio* energy of the products HCO^+ and NH_3 plus the lower limit for the reverse barrier which was obtained from the translational energy release. The rate *vs* energy curve for TS3 was then calculated by RRKM using the calculated frequencies for reactant and transition state. The next step was to carry out a series of calculations for TS2 by varying its potential energy. The best fit with experiment was obtained using a value of 284 kJ mol^{-1}. A curve showing the competition between TS2 and TS3 is reproduced in Figure 7. It can be seen that a value of 2 (as in the metastable ion spectra) for the branching ratio is consistent with ions having internal energy in the range 284 ± 30 kJ mol^{-1}. In this range an average $k = 6.7 \times 10^4$ s^{-1} can be calculated for TS2. This is equivalent to a lifetime of 15 μs (see Experimental Section). The choice of 289 kJ mol^{-1} for TS3 is of course somewhat arbitrary. The important result is that the RRKM calculation shows that TS3 lies approximately 5 kJ mol^{-1} higher than TS2. Further calculations showed that this energy difference is only very little dependent on the choice of the exact value chosen for TS3.

A substantial deuterium isotope effect is observed upon the competition between TS2 and TS3. A branching ratio of approximately 10 is obtained by RRKM (Figure 8) after adjusting for differences in zero-point vibrational energies and using vibrational frequencies for the monodeuteriated (the deuterium on oxygen) species. This finding is in good agreement with the branching ratios of the FTMS experiments.

Before constructing the final potential energy diagram one important assumption has to be made: namely, that all O-protonated molecules which rearrange via TS3 fragment to give $HCO^+ + NH_3$ rather than the thermodynamically more stable $NH_4^+ + CO$. This will now be discussed. Two requirements are made:

(i) The first is that the energy of the products ($HCO^+ + NH_3$) is lower than that of TS3. This implies that the energy of TS3 is larger than the experimental heat of formation of ($HCO^+ + NH_3$), which is 263 kJ mol^{-1}. This point has already been discussed.

(ii) The second requirement is that the fragmentation process which gives rise to $HCO^+ + NH_3$ is dynamically specific in the sense that there is a route which leads directly from TS3 to the products without passing the region of the potential energy surface associated with structures **3**, **4**, and **11** + **12**. This can be rationalized by looking at the potential energy surface in the region around TS3. The imaginary frequency of the reaction coordinate ot TS3 was calculated by *ab initio* to be 1715 cm^{-1} (scaled), which means that the potential energy surface is very curved along the reaction trajectory in the neighborhood of the transition-state structure. The H atom which moves from O to N will consequently acquire a large momentum and kinetic energy after the transition state has been passed. The direction and the magnitude of this momentum which is transferred to the N upon encounter is probably such that the C–N bond will break before rearrangement and transfer of a proton from HCO^+ to NH_3 can take place.

Potential Energy Hypersurface of Protonated Formamide. On the basis of the theoretical calculations *and* the considerations made above, we conclude with the model of Figure 9. This model is consistent with all available experimental evidence. Formamide may be protonated either on the nitrogen atom or on the oxygen atom. Although the O-protonated isomer, **2**, is thermodynamically favored, proton transfer to formamide is a complicated dynamical process and both isomers are formed. The N-protonated molecule has a rather low barrier for fragmentation into $NH_4^+ + CO$. The O-protonated isomer has two possible fragmentation ways which have approximately the same activation energy. One pathway leads to water loss, while the other leads to loss of ammonia. The latter reaction proceeds via a transition

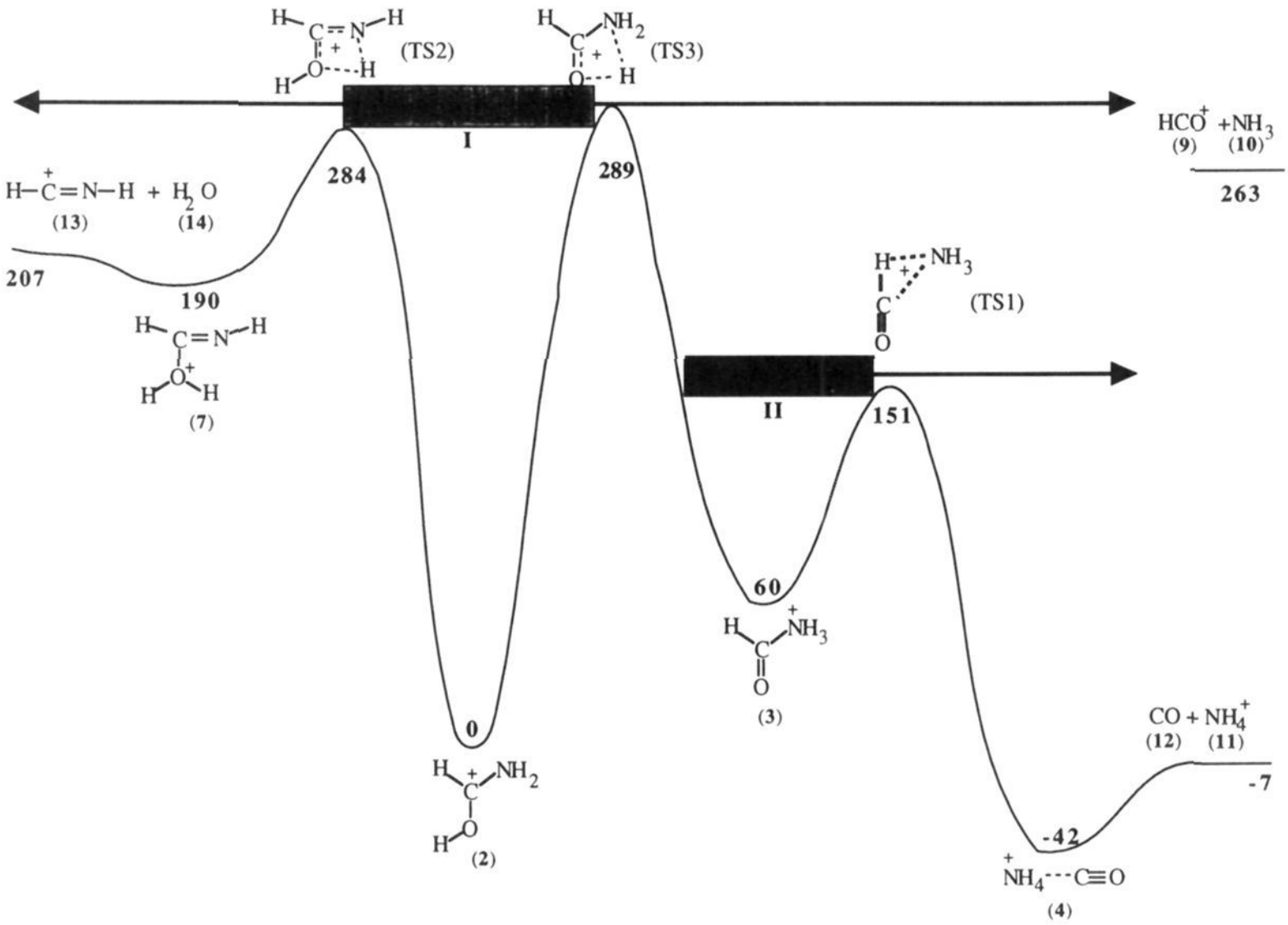

Figure 9. Theoretical potential energy diagram of the $(C,H_4,N,O)^+$ system. The diagram is based on the *ab initio* calculations. The barrier heights (TS2 and TS3) have been adjusted to be in better agreement with experiment.

state (TS3) which separates the two isomers of protonated formamide and must be nonstatistical due to the dynamical constraints of the preceding rearrangement. Otherwise, no loss of ammonia would take place because the competing reaction, loss of CO, is strongly favored.

The larger fraction of NH_4^+ ions formed from $(HCONH_2)H^+$ when CH_4 is used as the CI reagent gas than when H_2 is used may be explained by a larger tendency for production of O-protonated ions in energy range I (indicated in Figure 9) than N-protonated ions in energy range II. The factors which determine the dynamics, energetics, and site specificity of protonation are not yet fully understood.

Solution Chemistry. The question about the preferred site of protonation of amides in solution was open to controversy for a long time. Many spectroscopic methods were applied, and apparently contradictory conclusions were drawn. From all the evidence it appears that an O-protonated amide usually is more thermodynamically stable than the corresponding N-protonated isomer.[27] In other words, the intrinsic gas-phase base properties of amides are reflected in the solution phase. Although the O-protonated isomer is the dominating species, it is important to realize that small quantities of the N-protonated form are detected in weakly acidic solutions.

The fact that the O-protonated isomer is thermodynamically favored does not imply that the N-protonated isomer can be ruled out in the mechanisms of acid-catalyzed amide hydrolysis and proton exchange. Although the N-protonated isomer is less favorable thermodynamically, its rate of formation may be very fast. If a favorable reaction pathway exists from the N-protonated isomer, and not from the O-protonated isomer, the N-protonated species will be the observed intermediate.

Unfortunately, it appears that no mechanistic study of the hydrolysis of formamide in strongly acidic media has been performed. An S_N1-type A-1 mechanism would invoke formation of an intermediate formyl ion, HCO^+. As explained above, HCO^+ is only formed in the gas phase when the corresponding base of the proton donor is more than 263 kJ mol^{-1} less basic than formamide. This means that H_3O^+ is not sufficiently acidic (PA (H_2O) = 697 kJ mol^{-1}) to accommodate formation of HCO^+. If the gas-phase situation is transferrable to solution, this simply means that the A-1 mechanism can be ruled out for specific acid-catalyzed hydrolysis of formamide. Most amides seem to hydrolyze via the bimolecular mechanism (eqs 1a–d) even in strongly acidic solutions. In a series of amides and lactams investigated in various sulfuric acid concentrations,[28] only the β-lactam appears to hydrolyze via the unimolecular S_N1-type A-1 mechanism, probably because of the ring strain released upon formation of the acylium ion. Support for the bimolecular mechanism has also been found in the hydrolysis of acetamide in acetic acid.[29] Recent experimental and theoretical evidence has been presented which supports the bimolecular mechanism for acidic hydrolysis of formamide.[30]

Acknowledgment. E.U. wishes to thank the Norwegian Research Council (NAVF) and VISTA for the grants which made the trips to Newark ande Copenhagen possible.

(27) Giffney, C. J.; O'Connor, C. J. *J. Chem. Soc., Perkin Trans. 2* **1975**, 706.

(28) Cox, R. A.; Yates, K. *Can. J. Chem.* **1981**, *59*, 2853.
(29) Martin, R. J. L. *Aust. J. Chem.* **1965**, *18*, 807.
(30) Krug, J. P.; Popelier, P. L. A.; Bader, R. F. W. *J. Phys. Chem.* **1992**, 496, 7604.